THE BELL SYSTEM
TECHNICAL JOURNAL

VOLUME XXXIII SEPTEMBER 1954 NUMBER 5

Motion of Individual Domain Walls in a Nickel-Iron Ferrite

By J. K. GALT

(Manuscript received May 11, 1954)

Samples have been cut from single crystals of the nickel-iron ferrite $(NiO)_{0.75}$ $(FeO)_{0.25}Fe_2O_3$ *in such a way that they contain one and only one movable ferromagnetic domain wall. The viscous damping coefficient for this wall, which is a measure of the losses associated with domain wall motion in this material, has been measured as a function of temperature. This damping shows a very large increase as the temperature goes down to the region of 77°K. The value of this damping is correlated with the Landau-Lifshitz equation for the rotational motion of magnetization by means of previously available theoretical analysis. In addition, it is suggested that the sharp increase in damping at low temperatures is due to a relaxation associated with a rearrangement of the valence electrons on the divalent and trivalent iron ions in the ferrite. A tentative phenomenological theory of the losses based on this mechanism is presented.*

INTRODUCTION

The mechanism which contributes most to the permeability of high-permeability magnetic materials is the motion of ferromagnetic domain walls. These walls are thin lamellae in which the direction of the spontaneous magnetization of the material changes from one domain to another. As a result, this mechanism contributes a major part of the energy losses which accompany rapid changes in the direction of the

magnetization in such materials. In the ferromagnetic metals, it is well known that these losses ordinarily arise largely from the eddy currents which are induced by the motion of the domain walls. In the ferrites, however, the conductivity is so low that the contribution of eddy currents to the losses is never overwhelming and is often negligible; the losses must therefore in large part arise from other sources not yet understood. It is the purpose of this paper to present some recent studies of these losses and to discuss their relevance to the losses in ferrites generally.

In any ordinary sample of a ferromagnetic material, a study of domain wall motion and the associated energy losses is complicated by the fact that the domain pattern is very complex. Any attempt to provide a theoretical explanation of data taken on such samples must involve an averaging process over many domain walls of varying area, crystal orientation, etc. This makes it extremely difficult to describe the behavior of such patterns uniquely and quantitatively, although some progress has been made.[1,2] A method of avoiding this difficulty has been developed by Williams, Bozorth, Shockley, Kittel[3] and Stewart[3a] in working on silicon iron. This method consists in cutting a polygonal ring from a single crystal in such a way that each leg of the ring lies along one of the easy directions of magnetization in the crystal. In silicon iron this leads to a rectangular ring with each leg along a [100] crystal direction. In the ferrite which we use this technique to study here, the easy directions are [111] directions, and we use a diamond shaped sample as shown by the solid lines in Fig. 1. Each leg is along a [111] direction, and the major face is a (110) plane. If the sample is good enough, the domain pattern is that indicated by the dotted lines in Fig. 1. This pattern consists of four stationary walls, one at each corner, and one movable wall which goes all the way around the sample. The magnetization thus travels around the sample in two paths, one clockwise and the other counter-clockwise, and the position of the movable wall therefore determines the net circumferential magnetization. In such samples we study quantitatively and in some detail the motion of an individual movable wall.

Williams, Shockley and Kittel[3] studied the motion of the movable wall on one of the rectangles cut from a single crystal of silicon iron. They found the motion to be viscously damped, as Sixtus and Tonks[4] had in earlier experiments with more complicated domain walls. Because of the simplicity of their domain pattern, Williams, Shockley and Kittel were able to calculate the eddy current losses in their experiments, and to show that they accounted for most of the observed damp-

ing as expected. There was an additional contribution, however, which Kittel suggested was due to mechanisms of the sort which give rise to the width of ferromagnetic resonance lines.[5] These mechanisms of course are the controlling ones in the ferrites, where eddy current losses are small. The motion of a domain wall damped by such effects and unaffected by eddy currents was first discussed in a classic paper by Landau and Lifshitz.[6]

The experiments reported in the present paper consist of measurements of the velocity of a movable wall as a function of applied magnetic field in a sample like that shown in Fig. 1. The measurements are made by observing the voltage induced in a secondary winding on such a sample when a known field is applied by means of a pulse of current in a primary winding. The composition of the ferrites used in these studies is given by the approximate chemical formula $(NiO)_{0.75}(FeO)_{0.25}$-Fe_2O_3. Data have been taken as a function of temperature on several samples. The large, perfect crystals of the ferrites which are essential to the success of these experiments have been obtained through Dr.

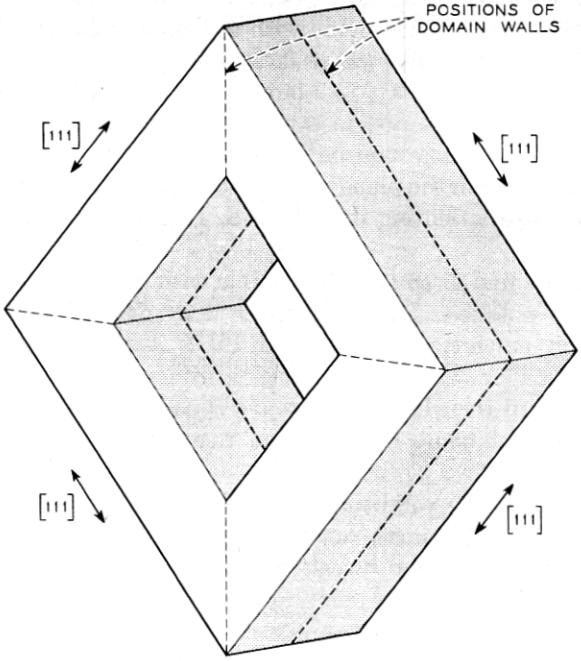

Fig. 1 — Sample of ferrite used in this study.

G. W. Clark from the Linde Air Products Company. Similar studies have been performed previously at room temperature on Fe_3O_4 [7] by the author, and in a preliminary way on $(NiO)_{0.91}$ $(FeO)_{0.09}$ Fe_2O_3 [8] by the author in collaboration with J. A. Andrus and H. G. Hopper.

THE EXPERIMENTS

Preparation of Samples

The key to the success of experiments of this sort is of course obtaining the domain pattern shown in Fig. 1, so that we have only one movable wall in the sample. The achievement of this pattern, and the observation of it when achieved, depend in turn on success in producing a perfect or almost perfect sample. It therefore seems worth while to describe the process which has finally emerged as a satisfactory way of producing these samples.

The rough crystal is first oriented by means of X-rays (Laue and X-ray goniometer techniques) to an accuracy of a few minutes while it is mounted in such a position that afterwards we can grind a flat on it which is coincident with the (110) plane. This flat is ground simply with a belt grinder. A cut is then made with a diamond saw parallel to this flat, so that we have a disc whose faces are (110) crystal planes. This disc is usually made about 2½ to 3 mm thick. The second face is ground accurately parallel to the first in a paralleling block. A flat coincident with the (100) plane is ground on the edge of this disc for later use in orienting the sample in the plane of the disc. This flat is also ground with a belt grinder after orienting the disc with Laue and X-ray goniometer techniques.

The disc is ground as smooth as possible with 303½ emery, and then very carefully polished. The polishing is done first on a lap surfaced with No. 0000 french emery paper, with Linde A abrasive loose on top of the emery paper. After this the lap is surfaced with a sheet of very smooth paper and then Linde B abrasive is used. The polishing process takes four to eight hours per disc, and removes all pits visible under 50× magnification, except those inherent in the crystal. Only on such a smooth surface can the very small holes which sometimes occur in these crystals be seen. Sometimes, however, the polishing process conceals fine cracks. It also cannot reveal variations in chemical composition which sometimes occur from point to point in the crystals. Such composition variations are presumably variations in the concentration of divalent iron from point to point in the crystal. In order to reveal these latter imperfections, the disc is etched for three hours by boiling it in

50 per cent H_2SO_4 under a reflux condenser. An asbestos pad is placed between the flame and the bottom of the flask containing the H_2SO_4 in order to prevent sharp temperature fluctuations in the bath. The rate of the etching attack, and the quality of the surface it leaves are sharply dependent upon temperature. It should be mentioned that if this etch is used on the discs *before* polishing, the surface remains rough or may even be made rougher, so that it is impossible to detect the imperfections in the disc. The etch must start on a smooth surface.

Once the disc is cut, polished, and etched, if it is found to be sufficiently free of imperfections, a sample is cut from it in such a way as to avoid those which there are, as they are revealed by the polishing and etching processes. First the diamond-shaped hole is cut by means of a jig whose rotational position with respect to the disc is determined from the (100) flat on the edge of the disc. This jig is a piece of steel which is driven in vibration vertically with a magnetostrictive drive.[9] The surface of the disc is covered with a slurry of carborundum or diamond dust, and this abrasive is made to cut a hole in the disc as the vibrating jig is slowly lowered. With the hole cut in the proper orientation, the outer parts of the disc are ground down to form the legs of the sample. Another jig of the proper shape is used to hold the sample in position during this process.

A hysteresis loop is taken as soon as the sample is cut. A relatively good loop taken on our best sample is shown in Fig. 2. All such loops on these samples are taken on the Cioffi recording fluxmeter.[10] This loop is obviously not yet in the form which we finally need. In order to square the hysteresis loop, we anneal the sample for approximately an hour at 600°C in a magnetic field of 10 to 20 oersteds. The field is produced by running a current through a few turns of glass insulated wire wound on the sample. After such a heat treatment the hysteresis loop of this sample assumed the form shown in Fig. 3.

Once the sample is prepared, the next problem is to observe the domain pattern and find if any important deviations from the pattern shown in Fig. 1 occur. The heat-treatment we give them corrodes the polished surfaces of the sample, and of course the faces exposed when the sample is cut from the disc have not yet been polished. Consequently both the major (110) faces of the sample and the outer faces of the legs are polished, and the sample is then etched in the same way as before. Usually a hysteresis loop is again taken at this point as a check. If the sample is good, it is not significantly different from the loop taken immediately after heat-treatment. The sample is brought to a demagnetized condition at this point so that the movable wall will be near the center of the sample where it can be observed. This completes the process of

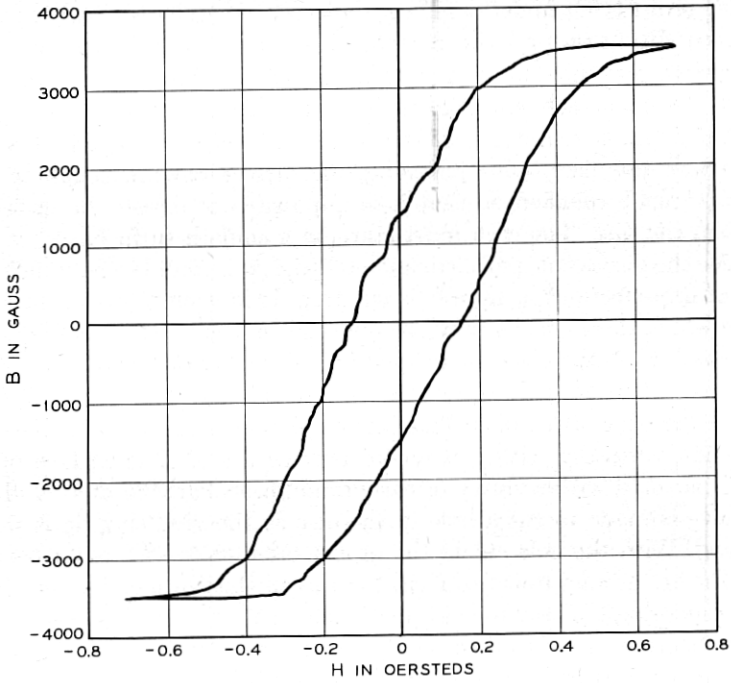

Fig. 2 — Hysteresis loop taken on sample before heat treatment in a magnetic field.

preparing the samples for observing their domain pattern and for performing our experiments on them.

Four samples have been prepared in this way for our studies on $(NiO)_{0.75}$ $(FeO)_{0.25}$ Fe_2O_3 .

Domain Pattern Observations

The method used to observe the domain walls on these surfaces is the same as that used by Williams and his collaborators.[3] We will therefore not describe it in detail. It consists essentially of observing through a microscope the pattern formed by a magnetic colloid on the surface.

The observation of domain patterns, even on these carefully prepared samples, is difficult. There is still some pitting on the surfaces. Also, many of the surfaces become rounded in the process of polishing. This produces surface spikes of the sort discussed by Williams, Bozorth and Shockley.[3] The result is that on many surfaces the domain pattern of the sample as a whole has to be discerned in a substantial amount

of extraneous structure such as surface spikes and pits. It is therefore impossible to show in one picture the whole pattern as diagrammed in Fig. 1. However, more detailed pictures of parts of the pattern do show that it is there. The essential features of the pattern on our best sample are shown in Figs. 4 and 5. Fig. 4 shows the stationary wall at one corner, and Fig. 5 shows a section of the movable wall on one leg. Differentiation of the domain walls in Figs. 4 and 5 from the many scratches is not very difficult after one has some experience in such observations.

The variation in wall position along the leg shown in Fig. 5 is due to the effects of strains and other imperfections, present even in this carefully prepared sample, in determining the position of the wall at rest.

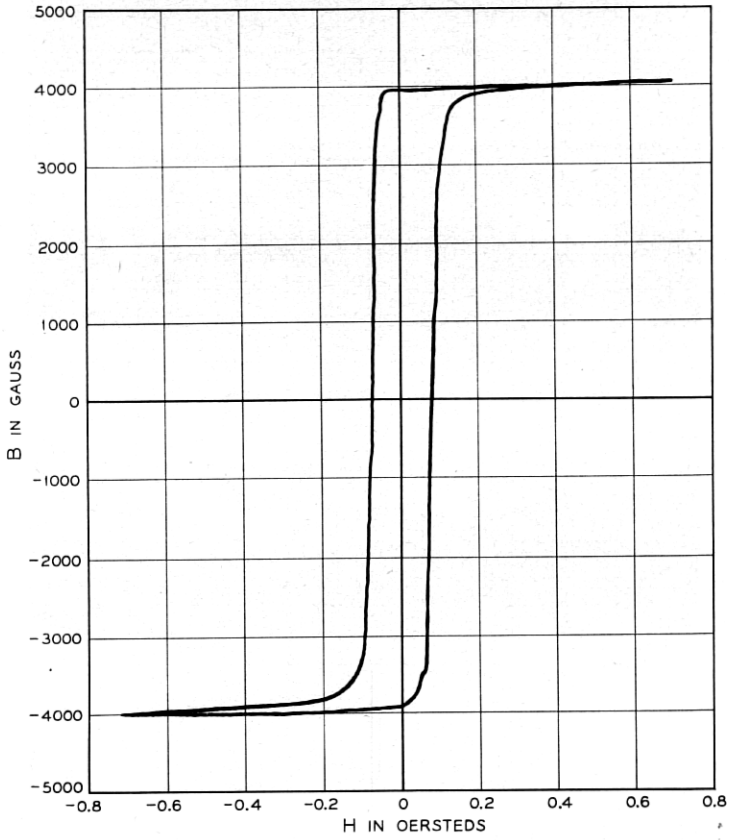

Fig. 3 — Hysteresis loop taken on same sample as loop in Fig. 2 after annealing for one hour at 580°C in a magnetic field of approximately 20 oersteds.

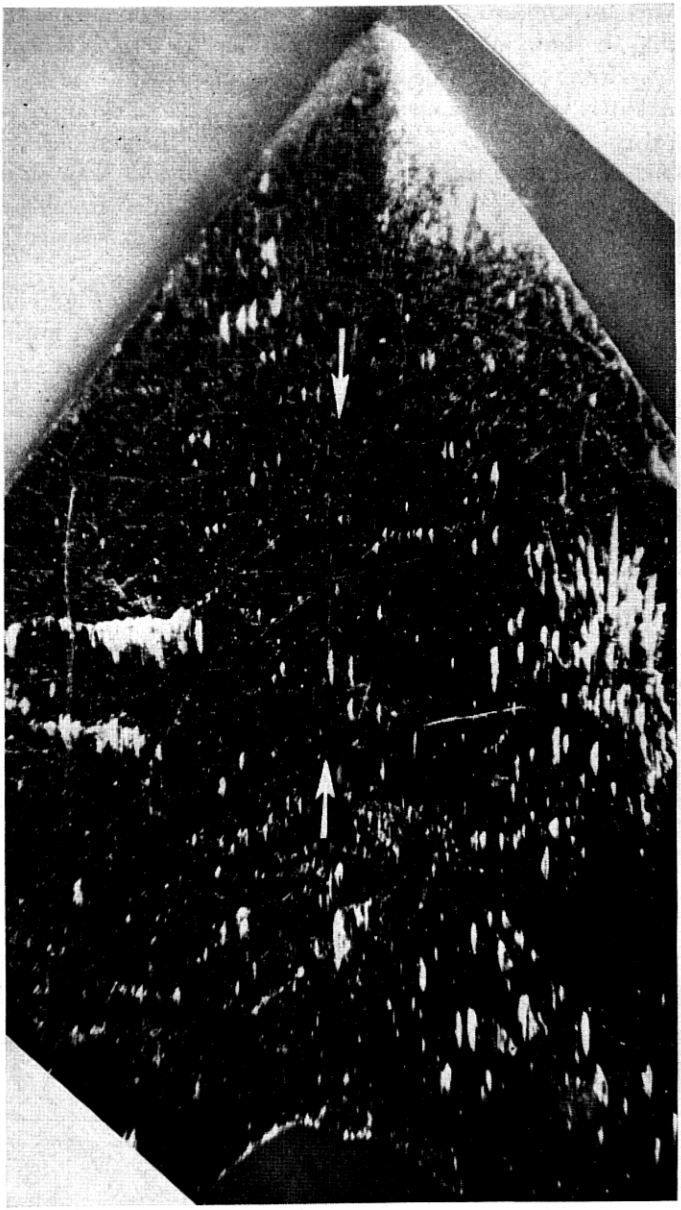

Fig. 4 — Picture of domain pattern at one corner of sample. The stationary wall is indicated by arrows.

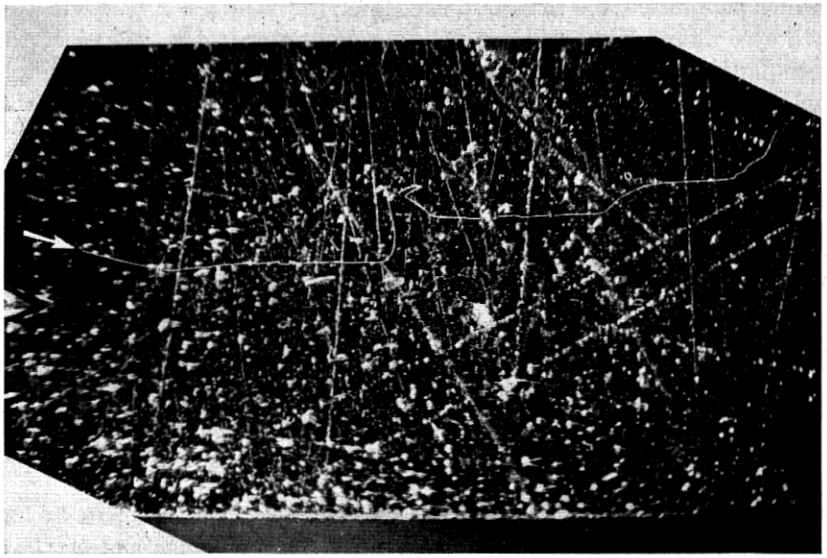

Fig. 5 — Picture of a section of the movable wall along one leg of sample. The line has been slightly emphasized by retouching after the picture was taken. The edge of the leg can be seen at the bottom of the figure.

It is unlikely that the wall is so distorted from a plane when in rapid motion, however, since then the driving force and the viscous damping resistance to motion are both much larger than the effects of these imperfections. The imperfections, of course, are primarily effective in determining the coercive force, as read from the hysteresis loop.

The domain pattern as traced out on each of four samples is discussed below:

Sample 1. Although they had spikes associated with them, the stationary walls expected at the corners could be seen, at least in part. In addition, at one of the acute angle corners there was some rather extensive domain wall structure. This structure had one form when the sample was magnetized in one direction, another when it was magnetized in the other. It was due to the presence of a small void at this corner whose magnetic energy was reduced by having domains of reversed magnetization around it. The existence of this void was established from structure which appeared in the spots on an X-ray Laue photograph taken at this point. The process of magnetization in this sample consisted in (a) the growth of the wall from the nucleus around this void until it existed all around the ring, and (b) the motion of this wall to the other side of the sample, where it again shrank to a configuration

which minimized the magnetic energy of the void. As a result of this state of affairs, the wall was not in equilibrium in the middle of the sample, but always shrank around the void so as to magnetize the sample in one direction or the other. It was impossible therefore to demagnetize the sample so that the wall was at the center of the legs and then have the wall stay there to be observed. The wall could be brought to the center, however, and held there using the technique mentioned by Williams and Shockley[3] (see Fig. 8 in their paper). The legs of the sample were so small that it was difficult to do this, but the wall was found on three legs of the sample at different times in this way. The wall curved a good deal in traveling along the legs. This sample was etched repeatedly so that data could be obtained as a fuction of sample dimensions. The variations observed led to a viscous domain wall damping independent of dimensions if it was assumed that the domain wall was perpendicular to the major (110) face. Therefore it was to this $(11\bar{2})$ plane that the wall was brought for observation.

Sample 2. Stationary walls at the corners were rather patchy but visible. The movable wall was traced along the outside faces of two legs, which indicates that it lay in the (110) plane. The wall curved a good deal. There were also other walls which enclosed patches of surface. It is suspected that these patches were the bases of spike domains extending into the sample from strain patterns on the surface. The sample was therefore etched again. Unfortunately, the bath apparently became locally overheated, and this etch took off rather more material than expected. It also left a matte surface on which domain walls could not be observed. The data taken on this sample, however, check those on other samples if we assume a pattern in which the movable wall is in the (110) plane, as our observations lead us to suspect.

Sample 3. The stationary walls at the corners were seen, but only with difficulty. They were patchy. There was a good deal of structure all along the legs on the major (110) face of this sample, but no wall which ran around the sample could be seen on this face.

On the outside of two of the legs, which are $(11\bar{2})$ faces, pitting and extraneous walls were so bad that the main wall could not be discerned. On a third, the wall could be traced most of the way. On the fourth, however, there were two walls, one of which could be traced along the whole leg, the other of which went only three-fourths of the way along the leg. Both walls on this leg showed a good deal of curvature. It therefore appears that the movable wall lies in the (110) plane, but that there is *another wall* big enough so that it may move and affect our data. This picture of a domain pattern with two movable walls was confirmed by checking the data obtained on this sample with those from others.

Sample 4. The stationary walls at the corners, although patchy, were seen. There was some extraneous domain wall structure on the major (110) faces, but nothing which looked at all like the main wall.

On the outside $(11\bar{2})$ faces of the legs, however, the wall was traced almost all the way around. Only short sections were impossible to trace. The wall curved as usual, and there was some extraneous domain wall structure on these faces, but substantially the whole of the ideal pattern shown in Fig. 1 was seen on this sample. The hysteresis loops shown in Figs. 2 and 3 and the domain pattern pictures shown in Figs. 4 and 5 were taken on this sample.

Not only was the domain pattern on sample 4 the best and most complete, but the data taken on this sample was much the most reproducible. We shall therefore report the data taken on this sample in detail, and simply refer to the results on other samples as a check and to indicate the sort of variations which occurred from sample to sample.

Measurements

Our procedure in making the measurements is as follows. The sample is wound with a primary and a secondary winding. A square pulse of positive voltage is applied to the primary winding in series with a resistor which is large enough to keep the pulse rise time short. The rise time must be short compared to the time required for the field produced by the pulse to reverse the magnetization of the sample. On the other hand, since the pulse is applied for the purpose of reversing the magnetization of the sample, the length of the pulse must be at least comparable with the time required for the reversal to occur; if possible, it should be longer than this. The reversal time, of course, is the time required for the mobile domain wall to move from one side of the sample to the other under the field produced by the applied pulse. A second pulse, of negative voltage, is applied to the primary during each cycle of the pulser in order to bring the wall back to its original position so that the phenomenon may be observed repetitively.

By synchronizing an oscilloscope sweep with the pulser, the signal induced in the secondary winding is observed while the applied pulse is on the primary. Since this signal is proportional to the velocity of the wall, it is constant to a first approximation during the application of a constant field. Irregularities in the crystal may cause the velocity of the wall to vary somewhat as it moves across the sample, however, and this will cause the signal to vary too. In this case, the observer reads the average value. Fig. 6 shows an example of the signal induced in the secondary winding as seen on an oscilloscope. Sample 4 was used to obtain this picture.

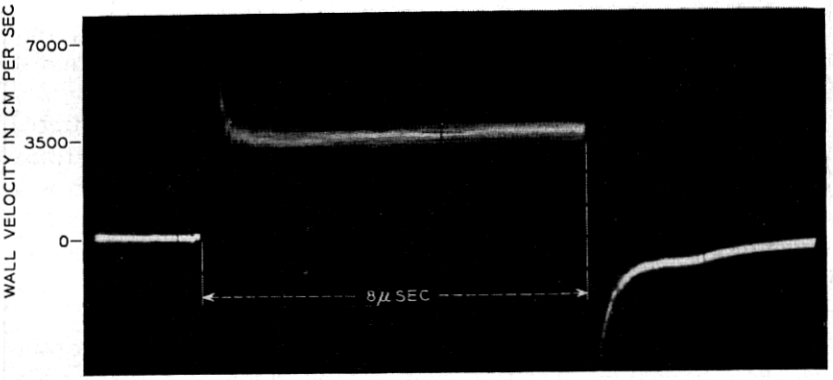

Fig. 6 — Oscilloscope trace of the induced voltage in the secondary winding while a square current pulse 8μ sec long was applied to the primary. The voltage spike at the beginning is not completely understood, but is thought to be connected with the fact that the domain wall spikes associated with imperfections do not pull back on the domain wall until it has moved a little distance. In this sample, once this initial peak is over, the wall velocity comes to its steady state value and is not much disturbed by imperfections, so that the observer need do no averaging. In this case, the wall was moving with a velocity of 3500 cm/sec. At this velocity, the wall was unable to reverse the magnetization in 8μ sec, so the signal ends as the magnetic field goes to zero at the end of the pulse. After the pressure on the wall due to the magnetic field stops, the domain wall spikes associated with imperfections pull the wall back slightly, giving rise to the voltage spike in the opposite direction.

The applied field due to the primary pulse is deduced from the current in the primary winding (measured by observing the voltage across the series resistor) using the solenoid formula $H = 4\pi NI$. To obtain the relation between wall velocity and induced voltage per secondary turn we have:

$$\text{Volts/turn} = (d\Phi/dt) \times 10^{-8} = 8\pi M_s(\Delta z/\Delta t)w_{\text{wall}} \times 10^{-8}, \quad (1)$$

where $(\Delta z/\Delta t)$ is equal to the domain wall velocity v, and w_{wall} is the width of the wall between the boundaries of the sample in the direction perpendicular to the direction of magnetization. It is in deriving (1), of course, that we use our detailed knowledge of the domain pattern in the sample.

We are thus able to obtain a value of the domain wall velocity v for each value of the applied field H. These data are the results of the experiment.

The value of M_s used in (1) is the measured value (322.5 cgs units/cc) at room temperature. The values used at other temperatures have been deduced on the assumption that M_s varies the same way with temperature in this material as it does in magnetite as measured by Weiss and

Forrer.[11] We have extrapolated their data to get the variation up to our highest temperatures.

In general, a plot of the data turns out to have the form shown in Fig. 7. This is the data taken on Sample 4 at 201°K. The wall does not move until the field exceeds the coercive force required to get it past various imperfections in the crystal. Its motion in fields higher than this is viscously damped. The wall velocity, v, therefore follows the relation:

$$v = G(H - H_c), \tag{2}$$

where H_c is the coercive field and G is the slope of the line drawn through the data. The value of G is high if the losses are low, and vice versa, of course.

RESULTS

Data on Sample 4 of the sort shown in Fig. 7 have been taken at various temperatures. We show in Fig. 8 a plot of $v/(H - H_c)$ as a function of temperature for this sample. Clearly, the outstanding feature of the data is a tremendous increase in the viscous damping of the domain wall at low temperatures.

Since the other samples were not as satisfactory, for reasons given above, we do not reproduce the data on them explicitly. Similar data have been taken on Samples 1 and 2, however, and they show the same behavior within their accuracy except that the very sharp decrease in $v/(H - H_c)$ seemed to occur at a somewhat higher temperature. This difference may be due to slight variations in composition among the

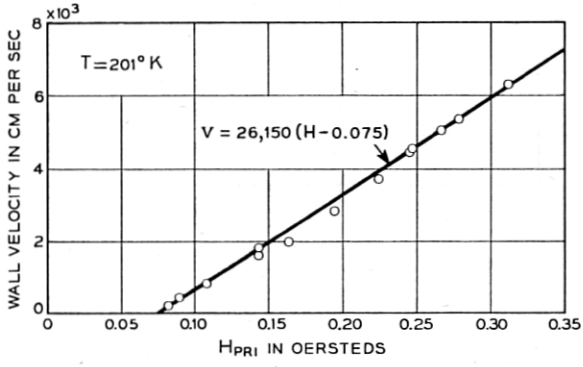

Fig. 7 — Typical plot of actual data for domain wall velocity as a function of applied field.

samples (Chemical analysis indicated that Sample 1 was

$$(NiO)_{0.77}(FeO)_{0.23}Fe_2O_3 ,$$

as distinct from

$$(NiO)_{0.75}(FeO)_{0.25}Fe_2O_3$$

for Sample 4) but it is possible that other more subtle differences such as the arrangement of the divalent nickel and iron ions are involved. Voltages induced in the secondary winding on Sample 3 for various applied fields were much higher than for the other samples at room temperature. This confirms the presence of more than one wall as indicated by the domain pattern. Therefore no further data were taken on this sample.

Each sample, after it had been cooled to the temperature of liquid

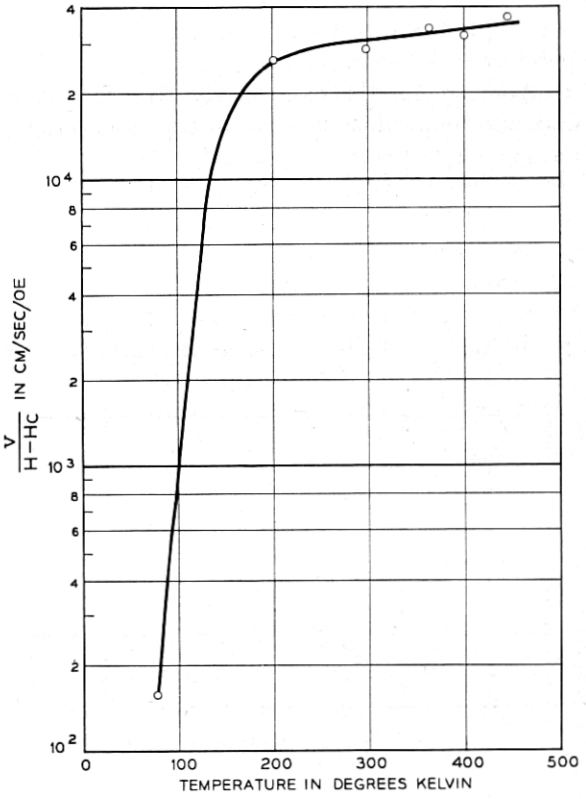

Fig. 8 — Plot of $v/(H - H_c)$ for Sample 4 as a function of temperature.

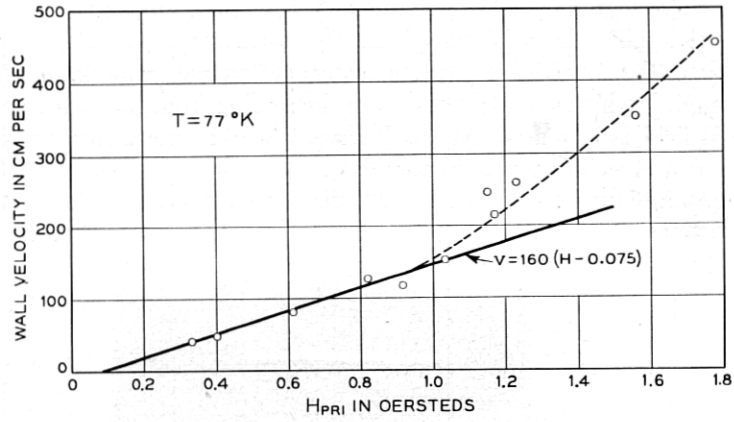

Fig. 9 — Plot of wall velocity as a function of applied field at 77°K. Note that at the higher fields the velocity is no longer a linear function of the applied field.

air once, gave the same value of $v/(H - H_c)$ as before. Samples 1 and 2, however, were cooled several times, and after the later runs they no longer did this. In both cases the value of $v/(H - H_c)$ as deduced from the ideal domain pattern and (1) was lower by about one-half; we interpret this to mean that the domain pattern in these samples was changed by the repeated thermal shock. Direct confirmation of this interpretation by observation was not possible, however, for reasons indicated above in connection with domain pattern observations on these samples.

In view of the fact that only one point is plotted beyond the knee of the curve in Fig. 8, it should be emphasized that continuous qualitative observations made while the sample was cooling showed that the change was continuous and monotonic. On Sample 1, furthermore, the data at 201°K was somewhat down from the knee of the curve [$v/(H - H_c) = 18000$ cm/sec/oe] because of the fact that the knee occurred at higher temperature as mentioned above.

Another feature of the data is indicated by Figs. 9 and 10. Data discussed thus far have been taken at the lowest convenient velocities in order to minimize the possibility of wall distortion. However, when data were taken at higher fields, a non-linearity of the sort shown in Fig. 9 appeared. The average velocity increases more rapidly at the higher fields than our viscous damping coefficient would lead us to expect. This effect was observed at all temperatures, but as comparison of Figs. 7 and 9 will show, it set in at lower velocities at low temperatures where the enlarged viscous damping appeared. Simultaneously with the appearance of this non-linearity in the apparent average velocity of the

wall, the voltage induced in the secondary winding during the pulse of constant applied field is seen from the oscilloscope trace to distort with time. Fig. 10 shows a series of traces observed at room temperature on Sample 4 which show this distortion increasing from (a) to (d) as the applied field is increased. At the highest fields the trace forms a peak which is almost triangular in shape.

We shall discuss the theoretical implications of these data in the next two sections.

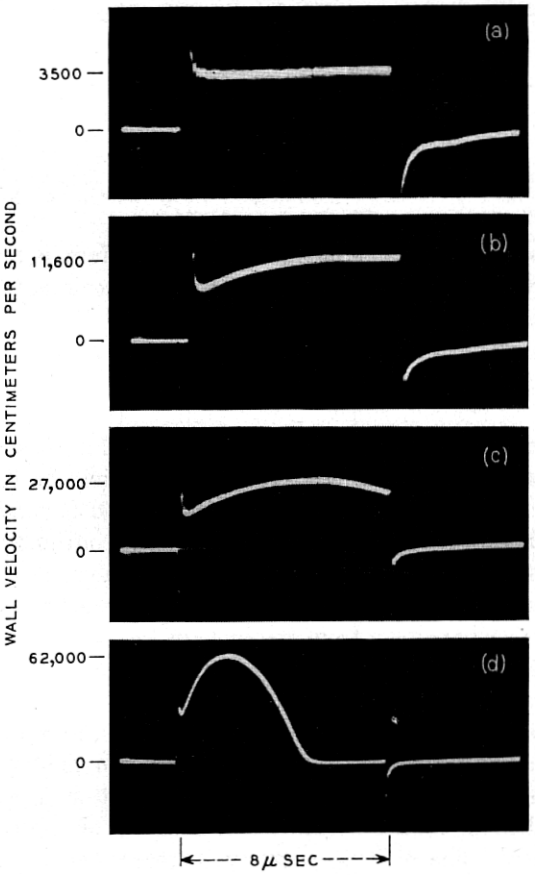

Fig. 10 — A series of oscilloscope traces showing the deviation of the wall velocity from a constant with time at the higher applied magnetic fields and therefore at the higher velocities. These pictures were taken at room temperature, but similar phenomena occur at all other temperatures in the range of applied fields where the nonlinearity in velocity shown in Fig. 9 becomes apparent. The velocities, as shown, increase from *a* to *d*.

THEORY

A theoretical analysis of the experimental results given in the last section divides itself rather naturally into three parts. First we characterize the data in terms of an equation of motion for unit area of domain wall. This means we determine the constants of motion (viscous resistance and coercive force in our case) of unit area of wall. Secondly, we show the relation between the viscous resistance of unit area of domain wall, and the constants which characterize the ferromagnetic material in general (saturation magnetization, crystal anisotropy, etc.). This is essentially an application of the recent work of Becker[12] and Kittel.[13] Lastly, we calculate the magnitude of the damping from a relaxation mechanism which accounts for the low temperature effect shown in Fig. 8 at least qualitatively.

Consider unit area of a 180° domain wall between two regions of saturated material. Such a system has an equation of motion for small amplitudes of the applied magnetic field H which may be written:

$$m\ddot{z} + \beta\dot{z} + \alpha z = 2M_sH, \tag{3}$$

where z is the displacement of the domain wall along its normal, m is its mass per unit area, β is a parameter measuring viscous resistance, and α is a stiffness parameter which has meaning only for small fields such as those used in initial permeability measurements. When fields larger than the coercive force are applied, as in our experiments, the term containing α disappears and the field effective in moving the wall is less than the applied field by an amount equal to the coercive force; this is shown by the data given previously in the section on results. This reformulation of (3) is quite reasonable when one remembers the spikes which pull back on the wall, in the experiments of Williams and Shockley, for small wall motions and snap off entirely if the wall moves a large distance. Furthermore, since the velocity of the domain wall rises to its steady value in a negligible time in these experiments (Fig. 6) the initial term in (3) is also negligible. As these remarks indicate, under the conditions of the experiment in wall velocity, (2) takes the form:

$$\beta\dot{z} = 2M_s(H_{\text{app}} - H_c). \tag{4}$$

This relation obviously fits the data given previously.

The second step in the theoretical analysis starts from an equation of motion for the magnetization $\vec{M}$ in a small volume which was first used by Landau and Lifshitz,[6] and takes advantage of more recent work of Becker[12] and Kittel.[13] If we consider a volume small enough so that the

magnetization in it is everywhere uniform even if we are inside the domain wall, our equation of motion is:

$$\frac{d\vec{M}}{dt} = \gamma[\vec{M} \times \vec{H}] - \lambda/M^2[\vec{M} \times (\vec{M} \times \vec{H})]. \tag{5}$$

Here γ is the gyromagnetic ratio ($ge/2$ mc), and λ is a parameter, assumed to be characteristic of a given ferromagnetic material, which is determined by the magnitude of the damping effects in the motion of $\vec{M}$. The magnitude of the last term on the right in (5) is thus determined by the amount of the damping losses.

The rate of dissipation of energy in the small volume is $\vec{H} \cdot (d\vec{M}/dt)$, where $\vec{M}$ is the magnetic moment of the volume, and $\vec{H}$ is the total magnetic field in the volume. The value of $\vec{H}$ requires some discussion. Outside the wall $\vec{H} = \vec{H}_0$ where $\vec{H}_0$ is the applied field, which is parallel to the wall. When the wall is moving, however, there is an additional field $\vec{H}_e$ inside it. This field, which is normal to the wall, is a demagnetizing field which arises from the tendency of $\vec{M}$ in the moving wall to have a component normal to the wall. This field has just such a value that the magnetization in the moving wall precesses about it with the Larmor frequency. Its value is:

$$\vec{H}_e = -(\vec{v}/\gamma)(\partial\theta/\partial z), \tag{6}$$

as Becker[12] has shown. Here $\vec{v}$ is the velocity of the wall, z is a distance coordinate normal to the wall, and θ is the rotational angle of the magnetization as we pass through the wall along z. Inside the wall, $\vec{H}_e$ is much larger than $\vec{H}_0$, but in any case $\vec{H} = \vec{H}_e + \vec{H}_0$. From (5) we find:

$$\vec{H} \cdot d\vec{M}/dt \cong \lambda H_e^2, \tag{7}$$

as Kittel[13] first showed. In the theory of the domain wall it is shown that $\partial\theta/\partial z$ in the wall is equal to the square root of the ratio of the increase in anisotropy energy as the magnetization turns away from the easy direction of magnetization, to the exchange energy constant. That is[14]:

$$\frac{\partial\theta}{\partial z} = ([g(\theta) - g(\theta_0)]/A)^{1/2}. \tag{8}$$

The exchange energy constant A is defined by the following expression for the exchange energy per unit volume due to gradients in the direction

of magnetization:

$$\text{Exchange energy/unit vol} = A[(\nabla\alpha_1)^2 + (\nabla\alpha_2)^2 + (\nabla\alpha_3)^2], \quad (9)$$

where α_1, α_2, and α_3 are the direction cosines of the magnetization. $g(\theta)$ is the anisotropy energy:

$$g(\theta) = K_1(\alpha_1^2\alpha_2^2 + \alpha_2^2\alpha_3^2 + \alpha_3^2\alpha_1^2), \quad (10)$$

expressed in terms of θ, and $g(\theta_0)$ is the anisotropy energy along the direction of easy magnetization. Note that $[g(\theta) - g(\theta_0)]$ is always positive. K_1 is the first order anisotropy constant.

If we use (6) and (8) in (7), and integrate over z along a cylinder of unit cross-section normal to the wall to get the rate of energy dissipation for unit area of moving wall, we have:

$$\int_{-\infty}^{\infty} \vec{H} \cdot \frac{d\vec{M}}{dt}\, dz = (\lambda v^2/\gamma^2 A^{1/2}) \int_{\theta_1}^{\theta_2} [g(\theta) - g(\theta_0)]^{1/2}\, d\theta = 2H_0 M_s v, \quad (11)$$

where θ_1 and θ_2 are the angular positions of $\vec{M}$ on the two sides of the wall. $\theta_2 - \theta_1 = \pi$, of course, since we are considering a 180° domain wall. In order to obtain (11), we have used (8) to transform from integration over z to integration over θ as well as to evaluate (7). We set our result equal to $2M_sH$ (pressure on the wall) times v since this is the rate at which the wall, considered phenomenologically, does work. We may now write:

$$v = \frac{2M_s\gamma^2 A^{1/2}}{\lambda \int_{\theta_1}^{\theta_2} [g(\theta) - g(\theta_0)]^{1/2}\, d\theta} H_0. \quad (12)$$

This is the desired relation between wall velocity and applied field which is to be compared with (4). In this way we find:

$$\beta = (\lambda/\gamma^2 A^{1/2}) \int_{\theta_1}^{\theta_2} [g(\theta) - g(\theta_0)]^{1/2}\, d\theta. \quad (13)$$

We have thus shown the relation between the wall parameter β and the parameter λ which measures in general the losses associated with motions of the magnetization.

The third part of our theoretical analysis is concerned with a calculation of the damping parameter λ, or rather the relation between v and H itself, from an explicit physical mechanism. Such a calculation has not been made in the past since the appropriate mechanism on which to base it has remained obscure. Verwey and his co-workers[15] have explained the well known transition at about 115°K in Fe_3O_4 as

an order-disorder transition in the arrangement of the divalent and trivalent iron ions. M. Fine of Bell Telephone Laboratories has found a remnant of this transition in crystals of the same composition as those studied in the present research, by means of ultrasonic measurements of elastic constants.[16] We propose that the mechanism which causes the sharp rise in the damping of domain wall motion at low temperatures is a relaxation associated with this transition. Wijn and van der Heide[17] have explained in this way observations of theirs of losses associated with initial permeability at low frequencies in certain other polycrystalline ferrites. The time associated with this relaxation should be short because this rearrangement of ions involves only the motion of electrons from one site to another.[18] It should be of the order of the relaxation time associated with the electrical conductivity of Fe_3O_4. Snoek[19] has suggested some time ago that losses in the ferrites were due to an after-effect (relaxation) which, because of the short time constant involved, must be associated with electron migrations.

It is extremely useful to compare our data with a theory of the damping based on the above relaxation mechanism no matter what assumptions we make in detail about what it is that relaxes. We shall see that we are led quite generally to the result that $v/H \sim 1/\tau$ where τ is the relaxation time for the process. However, in order to perform this calculation explicitly we must make more detailed assumptions about exactly what quantity relaxes with the relaxation time τ. Changes in the direction of the magnetization cause changes in stress in the sample because of magnetostriction. One possible assumption is that the resulting strain would lag behind this stress and mechanical energy would be dissipated in the crystal. This mechanism, however, cannot act in our case. The magnetization in the two domains on each side of the wall points in opposite directions, but causes the same strain in both, and they have such a large stiffness that the thin region occupied by the domain wall assumes this same strain even though the direction of the magnetization is different there. Thus regardless of the stresses produced in the wall, the strains remain the same, inside and outside the wall, whether it is moving or not; under these conditions no work is done on the lattice, and no energy can be lost in this way by the moving wall. A calculation has been made by the author on the assumption that it is the magnetization itself which relaxes with relaxation time τ. This assumption leads to the result that wall velocity is *not* linearly dependent upon $(H - H_c)$; it is therefore not correct, since the data shows such a linear dependence. A similar result is to be expected if we assume that the dielectric polarization relaxes.

What seems at present likely to be the approximate nature of the mechanism, and what we will assume is the nature of the mechanism for the purposes of an illustrative calculation is as follows. As the domain wall passes a point in space, and the direction of $\vec{M}$ changes, the electrons on the divalent and trivalent iron ions tend to rearrange themselves so as to minimize the magnetocrystalline anistropy energy.[20] If $\vec{M}$ changes slowly this anistropy energy is near the minimum possible value (the *reversible* value) at all times, and the process is almost isothermal. As a result of the fact that the process deviates irreversibly from equilibrium, however, net work is done in bringing about the change. If, on the other hand, the direction of $\vec{M}$ changes so suddenly that the electrons have no time to rearrange, the process is adiabatic, and the magnetocrystalline anistropy energy varies more widely with the angular position of $\vec{M}$.

Since our data is taken at low velocities and extrapolated to zero velocity, it seems most appropriate for us to make a calculation of the losses on the assumption that as we increase the velocity of the wall we are deviating from the isothermal condition. Let us define as a thermodynamical system the part of the magnetic lattice which lies in a small volume fixed in space. This volume is a sheet of unit cross-section in which the magnetization is uniform and which is part of the cylinder of unit cross-section normal to the wall mentioned in connection with (11). From the first law of thermodynamics, as the wall passes the small volume, we have:

$$dw = dU - dQ = dg, \tag{14}$$

where dQ is heat added to the system, dU is a change in internal energy, dw is work done on the system, and g is the anisotropy energy associated with our rearranging electrons. Note that g, is a term in the free energy of the magnetic lattice. The free energy includes other terms in addition to g, and indeed there is in general another term in the magnetocrystalline anistropy energy; we will not consider any of these, however, since they also integrate to zero as the domain wall passes our small volume. Similarly, there are many contributions to dw, but we will concern ourselves only with the term which does net work on our system, the pressure on the wall times its velocity. If we now consider changes in our system with time we have from (14):

$$\frac{dw}{dt} = \frac{dg}{dt}. \tag{15}$$

The rate of doing work on unit area of the wall moving along our

cylinder, which is the integral of dw/dt over the cylinder, is $2M_sH_0v$ as in (11). The rate of dissipation of energy in this section of the wall is somewhat more difficult to calculate. It is the sum of contributions from all the small volumes along the cylinder. In order to calculate the contribution from the small volume we are considering, we first note that if the process is reversible,

$$dg = \frac{dg}{d\theta}\, d\theta, \tag{16}$$

where θ is the angle of rotation of $\vec{M}$. Physically, the factor $dg/d\theta$ represents a torque on the magnetization. We will assume that (16) holds even when the domain wall passes our system at a finite velocity and we have departed slightly from isothermal equilibrium. The field H_e defined in (6) transmits this torque to make the magnetization rotate through the angle θ, but we will not go further into the details of this process.

As the domain wall goes by, $dg/d\theta$, which we will abbreviate as g', changes. If the process were reversible, g' would be zero at all times and the torque on the magnetization would always have its equilibrium value. Actually, as we deviate more and more from the reversible process by moving the wall faster, the electrons are no longer able to rearrange fast enough, and g' deviates from zero while continually relaxing toward it. We must form our analysis in such a way that a maximum is established for g', since even if the magnetization moves infinitely rapidly, g' does not become infinite. Since the electrons minimize their free energy, it must be positive, and we write $g = g_{1\infty} - g_1$ so that $g' = g'_{1\infty} - g'_1$, where g'_1 relaxes toward $g'_{1\infty}$. Note that the torque relaxes *downward* from a value, $g'_{1\infty}$, associated with the adiabatic anisotropy energy (fast motions of the magnetization) to a value zero, associated with the isothermal anisotropy energy (slow motions of the magnetization). We may now write:

$$\frac{dg'_1}{dt} = \frac{g'_{1\infty} - g'_1}{\tau}. \tag{17}$$

Physically, this relation assumes that the torque on the magnetization relaxes in the same way if $g'_{1\infty}$ is a continuous function of time as it would if $g'_{1\infty}$ and g'_1 differed but $g'_{1\infty}$ was constant. Here τ is the relaxation time associated with the rearrangement of divalent and trivalent iron ions. If we write (17) in the form:

$$\frac{dg'_1}{dt} + \frac{g'_1}{\tau} = \frac{g'_{1\infty}}{\tau}, \tag{18}$$

we see at once that the solution for g_1' as a function of t as the domain wall passes the position of our small volume is:

$$g_1'(t) = \frac{1}{\tau} e^{-t/\tau} \int g_{1\infty}'(t) e^{t/\tau}\, dt. \tag{19}$$

We have ignored the solution of the homogeneous equation, as it contains a factor $e^{-t/\tau}$.

In order to evaluate (15) for our small volume, we need a more explicit value for g_1'. From the Fourier transformation we may write:

$$g_{1\infty}'(t) = \int_{-\infty}^{\infty} G_{1\infty}'(\omega) e^{i\omega t}\, d\omega. \tag{20}$$

Consequently:

$$g_1'(t) = \frac{1}{\tau} e^{-t/\tau} \iint_{-\infty}^{\infty} G_{1\infty}'(\omega) e^{(1/\tau + i\omega)t}\, d\omega\, dt. \tag{21}$$

This can be integrated over t. If we do this, then bring the factor $e^{t/\tau}$ out from under the integral sign, we find:

$$g_1'(t) = \int_{-\infty}^{\infty} \frac{G_{1\infty}'(\omega)}{1 + i\omega\tau} e^{i\omega t}\, d\omega. \tag{22}$$

Now the frequencies for which we get a contribution to the integral in (22) have an upper bound determined by the velocity and the thickness of the domain wall, of course. The faster the domain wall moves, the higher the upper bound on the frequency. We have been careful to make our measurements near zero wall velocity, and the data clearly extrapolates linearly to zero. This was done in order to minimize the possibility of wall distortion, but it also is consistent with our assumption of almost isothermal conditions. We are therefore justified in assuming that $\omega\tau \ll 1$ for all the frequencies in $G_{1\infty}'(\omega)$, and we can expand the factor $1/(1 + i\omega\tau)$ in (22). We obtain:

$$g_1'(t) = \int_{-\infty}^{\infty} [1 - (i\omega\tau) + (i\omega\tau)^2 + \cdots] G_{1\infty}'(\omega) e^{i\omega t}\, d\omega, \tag{23}$$

and if we form the derivatives of (20) and compare them with the terms in (23), we see that:

$$g_1'(t) = g_{1\infty}'(t) - \tau \frac{dg_{1\infty}'(t)}{dt} + \tau^2 \frac{d^2 g_{1\infty}'(t)}{dt^2} + \cdots \tag{24}$$

Since the value of τ is very much less than one, the series in (24) converges quite rapidly at low domain wall velocities, and we only keep the first two terms.

Until now, we have been concerned with a small volume of the magnetic lattice fixed in space. As in deriving (11), if we wish to calculate the rate of loss of energy for unit area of the domain wall moving with constant velocity, we must integrate dg_1/dt over a cylinder of unit cross-section normal to the wall. $g'_{1\infty}$ is now a function of $(t - z/v)$ where v is the velocity of the domain wall, and z is a coordinate normal to the wall. If we form this integral, and use (16) and (24), we find:

$$\int_{-\infty}^{\infty} \frac{dg_1}{dt}\, dz = \int_{-\infty}^{\infty} \left[g'_{1\infty}(t - z/v) - \tau \frac{dg'_{1\infty}}{dt}(t - z/v) \right] \frac{d\theta(t - z/v)}{dt}\, dz \quad (25)$$

We note that:

$$\begin{aligned} \frac{dg'_{1\infty}(t - z/v)}{dt} &= -v \frac{dg'_{1\infty}(t - z/v)}{dz}, \\ \frac{d\theta(t - z/v)}{dt} &= -v \frac{d\theta(t - z/v)}{dz}. \end{aligned} \quad (26)$$

For the first term in (25) we find, using (26):

$$\int_{-\infty}^{\infty} g'_{1\infty}(t - z/v) \frac{d\theta(t - z/v)}{dt}\, dz = -v \int_{\theta_1}^{\theta_2} g'_{1\infty}(t - z/v)\, d\theta = 0, \quad (27)$$

since $g_{1\infty}$ is the same on both sides of the domain wall. Now if we use (26) in the second term of (25), and remember the result in (27), we have:

$$\int_{-\infty}^{\infty} \frac{dg_1}{dt}\, dz = -\tau v^2 \int_{-\infty}^{\infty} \frac{dg'_{1\infty}(t - z/v)}{dz} \frac{d\theta(t - z/v)}{dz}\, dz. \quad (28)$$

We may, without loss of generality, evaluate the intergral in (28) at $t = 0$. It is therefore the integral of a function of z over z. In order to evaluate it, we wish to express $g'_{1\infty}$ as a function of θ. We have:

$$\int_{-\infty}^{\infty} \frac{dg_1}{dt}\, dz = -\tau v^2 \int_{-\infty}^{\infty} \frac{dg'_{1\infty}}{d\theta} \left(\frac{d\theta}{dz} \right)^2 dz, \quad (29)$$

$$= -\tau v^2 \int_{\theta_1}^{\theta_2} \frac{d^2 g_{1\infty}}{d\theta^2} \frac{d\theta}{dz}\, d\theta, \quad (30)$$

where we have replaced $g'_{1\infty}$ by $dg_{1\infty}/d\theta$. We note now, from the relation between g and g_1, that $dg_1/dt = -dg/dt$. We therefore set the right hand

side of (30) with reversed sign equal to:

$$\int_{-\infty}^{\infty} \frac{dw}{dt}\, dz = 2M_s H_0 v,$$

as mentioned after (15) to get the relation between the velocity of the domain wall and the applied field. As we shall see later, the right hand side of (30) is positive if we use a $g_{1\infty}$ associated with a positive contribution to the anisotropy energy. We find:

$$v = \frac{1}{\tau} \frac{2M_s}{\int_{\theta_1}^{\theta_2} \frac{d^2 g_{1\infty}}{d\theta^2} \frac{d\theta}{dz}\, d\theta} H_0 . \tag{31}$$

The derivatives of θ with respect to z in (29), (30), and (31) are to be evaluated by means of (8) and (10). In using these equations, of course, we are assuming that the wall is moving slowly enough so that its shape remains that of the wall at rest.

Equation (31) shows that $v \sim H/\tau$ as we mentioned earlier. Inspection of Fig. 8 shows that this relationship explains very satisfactorily the sharp drop in $v/(H - H_c)$ at low temperatures if we remember that τ depends on temperature as follows:

$$\tau = \tau_\infty e^{\epsilon/kT}, \tag{32}$$

where ϵ is an activation energy.

Finally, the right hand side of (30) may be set equal to:

$$\int_{-\infty}^{\infty} (\vec{H} \cdot d\vec{M}/dt)\, dz,$$

as calculated from the Landau-Lifshitz equation, see (11), to obtain a value for λ. We find:

$$\lambda = \tau \frac{\gamma^2 A^{1/2} \int_{\theta_1}^{\theta_2} \frac{d^2 g_{1\infty}}{d\theta^2} \frac{d\theta}{dz}\, d\theta}{\int_{\theta_1}^{\theta_2} [g(\theta) - g(\theta_0)]^{1/2}\, d\theta} . \tag{33}$$

DISCUSSION

It is clear that (4) fits our experimental data at each temperature. By fitting our data to this expression we obtain values for β, the parameter characteristic of the material which measures the damping of the wall. Values of β obtained in this way are given in Table I. A more

correct value of M_s for Fe_3O_4 at room temperature (475 c.g.s. units) has been used in calculating the β given in Table I than has been used in previous calculations.

In Table I we give in addition to values of β, values of λ at room temperature obtained from (13). The value for Fe_3O_4 is calculated from the new value of β and also corrected for the error mentioned in Reference 14. Values given in References 7 and 8 are somewhat in error. The values of β and λ given for Fe_3O_4 in Table I are the remainders after the contribution due to eddy currents has been subtracted out by means of the low field calculation of Williams, Shockley, and Kittel,[3] [see their Equation (11)].

TABLE I — ROOM TEMPERATURE DATA ON Fe_3O_4 AND $(NiO)_{0.75}\,(FeO)_{0.25}\,Fe_2O_3$

	(c.g.s. units)		
	β (corrected for eddy currents)	λ domain wall	λ ferromagnetic resonance
Fe_3O_4	0.44	5.5×10^8	9×10^8
$(NiO)_{0.75}\,(FeO)_{0.25}\,Fe_2O_3$	0.023	4.6×10^7	10×10^7

TABLE II — DATA FOR $(NiO)_{0.75}\,(FeO)_{0.25}\,Fe_2O_3$*

T(°K)	M_s (c.g.s. units)	K_1 (ergs/cc)	$v/(H - H_c)$ (cm/sec/oe)	λ domain wall (c.g.s. units)
77	341	-8.1×10^4	158	6.3×10^9
201	335	-5.4×10^4	26150	4.4×10^7
300	322.5	-3.8×10^4	28500	4.6×10^7
363	309	-3.1×10^4	32500–35300	4.0–4.3×10^7
400	298	-2.8×10^4	31750	4.5×10^7
445	281	-2.4×10^4	36850	3.9×10^7

* The value of M_s at 300°K is measured from the hysteresis loop of Fig. 3. Other values were obtained by assuming that M_s varied with T in the same way as observed by Weiss and Forrer[11] in Fe_3O_4.

The evaluation of λ from (13) is done as follows. Since the wall is in a (110) plane, we find from (10):

$$g(\theta) - g(\theta_0) = \frac{|K_1|}{4}\,(2/\sqrt{3} - \sqrt{3}\sin^2\theta)^2, \tag{34}$$

where θ is the angle between $\vec{M}$ and the [100] direction which lies in the plane of the domain wall. θ is $\cos^{-1}(1/\sqrt{3})$ on one side of the wall, and

$\pi + \cos^{-1} 1(/\sqrt{3})$ on the other. Then,

$$\int_{\cos^{-1}(1/\sqrt{3})}^{\pi+\cos^{-1}(1/\sqrt{3})} [g(\theta) - g(\theta_0)]^{1/2}\, d\theta = 0.92 \sqrt{|K_1|}\,. \tag{35}$$

In performing this integration, care must be taken to use the positive value of the square root over the whole interval. It should be noted that in using (8) and (10) to evaluate (13) we are assuming that the wall is moving slowly enough so that its shape is the same as that of the wall at rest. A is best evaluated from a fundamental relation derived by Herring and Kittel[21] between A and the Bloch constant:

$$A = [S_0/\Omega]^{1/3}[k/13.3C^{2/3}], \tag{36}$$

where k is Boltzmann's constant, C is Bloch's constant as used in the relation $M_s = M_0(1 - CT^{3/2})$, S_0 is the atomic spin, and Ω is the atomic volume. (S_0/Ω) is equal to the saturation magnetization at 0°K divided by twice the Bohr magneton.

For Fe_3O_4, we find $C = 4 \times 10^{-6}$ by fitting the Bloch $T^{3/2}$ law to the saturation magnetization measurements of Weiss and Forrer.[11] From (36), assuming M_s at 0^0K is 505 c.g.s. units, we then find $A = 1.24 \times 10^{-6}$. Furthermore, $K_1 = -1.1 \times 10^5$ as given by Bickford,[22] and

$$\gamma = (1.76 \times 10^7)g/2 = 1.865 \times 10^7,$$

where we have used Bickford's[22] value (2.12) of g.[23] Now from (13) we find

$$\lambda = 5.5 \times 10^8$$

in Fe_3O_4 at room temperature.

For $(NiO)_{0.75}(FeO)_{0.25}Fe_2O_3$, we assume that M_s, while different from that for Fe_3O_4, varies in the same way with temperature so that $C = 4 \times 10^{-6}$. From our measurement of M_s at room temperature (322.5 c.g.s. units) and this assumption about the variation of M_s with T, we find that M_s at 0°K is 342 c.g.s. units. This leads by (36) to $A = 1.09 \times 10^{-6}$. Ferromagnetic resonance experiments[24] done by W. A. Yager and F. R. Merritt in collaboration with the author on spherical single crystals of the same ferrite material as that used in the present research give a g value of 2.14 at all the temperatures mentioned in Table II except 77°K, where $g = 2.19$. These values are used in determining the value of $\gamma[= 1.76 \times 10^7\ g/2]$ in (13). The anisotropy values in Table II are also taken from the results of these ferromagnetic resonance experi-

ments. The K_1 at room temperature is -3.8×10^4. The room temperature value of λ domain wall given in Table I and the values at various temperatures given in Table II are obtained from (13) using these data.

An independent value of λ may be obtained from the ferromagnetic resonance line width. The relation between the observed line width $2\Delta H$ and λ has been given elsewhere.[25] Sample shape enters this relation, but not in a critical way, and we therefore ignore it except as it affects the value of the dc magnetic field at resonance, H_{res}. The relation is:

$$\lambda = \Delta H \gamma M_s / H_{\text{res}} . \tag{37}$$

From Bickford's[22] data on line width and (37) we find $\lambda = 9 \times 10^8$ for Fe_3O_4 at room temperature. From the ferromagnetic resonance data reported elsewhere[24] on $(NiO)_{0.75}(FeO)_{0.25}Fe_2O_3$, the material used in the present research, we find $\lambda \cong 10 \times 10^7$ at room temperature. Table I compares the room temperature values of λ obtained in the two ways on the two materials.

The differences between the domain wall experiments and the ferromagnetic resonance experiments lead to quite different behavior of λ in the two cases at low temperatures. These differences can be understood in terms of the frequency dependence of λ as given by an extension of the relaxation theory given in the third part of the theoretical discussion. A discussion of these relationships must await the detailed report on the ferromagnetic resonance results which is now in preparation, where such an extension will be given. As Table I shows, the room temperature values obtained in the two ways are of the same order of magnitude.

Let us now turn to a discussion of the relation between (31) and (33) and the data shown in Fig. 8. Qualitatively, of course, the $1/\tau$ factor in v/H_0 which (31) reveals, taken together with (32) explains most satisfactorily the sharp increase in viscous damping of the domain wall at low temperatures. Furthermore, it seems quite possible, although the author has not investigated it, that the higher order terms in (24) account for the nonlinearities in Figs. 9 and 10.

It should be mentioned that an increase in relaxation time at low temperatures which is consistent with (32) has been deduced by Bloembergen and Wang[26] and Healy[27] from ferromagnetic resonance data taken by them.

Quantitatively, we have inadequate data for a satisfactory comparison between Fig. 8 and (31), and the assumptions of the theory should perhaps be investigated further before any such comparison is taken

seriously. Nevertheless, plausible assumptions can be made which make an instructive comparison possible. $g_{1\infty}$ in (31) is equal to the difference in the variation of the anisotropy energy when measured adiabatically and when measured isothermally. At this stage of our knowledge, many assumptions which still retain the symmetry of the crystal are possible concerning the form of $g_{1\infty}(\theta)$. For our present purposes we will assume that it is given to within a constant by (34), but we must introduce a minus sign to take account of the fact that the rearranging electrons must have a *positive* anisotropy energy associated with them. Since we differentiate before substituting in (31), we do not need to subtract out the constant. The amplitude of $g_{1\infty}$ is not given by $|K_1|$ of course; we will call this amplitude $|K_r|$. When we introduce the minus sign into (34), and calculate the integral in (31), we find:

$$v = \frac{1}{\tau} \frac{4.0 M_s}{|K_r| \sqrt{\frac{|K_1|}{A}}} H_0 . \tag{38}$$

This relation points up the fact that the mechanism we are discussing here is characterized by two parameters, an amplitude factor $|K_r|$ and a time τ. Our experiment tells us nothing about $|K_r|$, so we will arbitrarily assume it is about ½ of $|K_1|$ at room temperature, or 20000 ergs/cc. $|K_r|$ can be measured by comparing values of $|K_1|$ determined isothermally, say by measuring the torque on a disc, and values of $|K_1|$ determined adiabatically, say by ferromagnetic resonance experiments, but this has not been done as yet. To determine τ at 77°K, assume that the maximum frequency of rotation of dipoles in the wall is such that $\omega\tau \leqq 0.1$ when the non-linearity shown in Fig. 9 first occurs (at $v = 150$ cm/sec). We calculate the thickness of the wall to be 4×10^{-5} cm from standard formulae (see Kittel's review article, Reference 14) and find $\tau \leqq 0.5 \times 10^{-8}$. These values of τ and $|K_r|$, together with $|K_1|$ from Table II at 77°K and A as calculated above, give $v/H_0 \leqq 40$ when inserted into (38). This is to be compared with a measured $v/(H - H_c)$ of 160 at 77°K. In view of the preliminary nature of (31), and the arbitrariness of some of our assumptions, this check is quite satisfactory. It would be naive to expect the theoretical result to be closer than an order of magnitude to the experimental one. Inspection of Fig. 8 suggests that the mechanism which gives the sharp increase in damping at 77°K is submerged at room temperature in the effects of other mechanisms, perhaps other electronic rearrangements, perhaps exchange effects of the sort recently suggested in metals by Rado.[28] Equation (39) confirms this expectation when we use $\tau \leqq 10^{-12}$, as determined either

from ferromagnetic resonance data[24] or from the conductivity of Fe_3O_4. The above method of calculating τ from domain wall data is less satisfactory at room temperature.

The idea of associating losses in ferrites such as this one with changes of order in the divalent and trivalent iron ions explains the fact that the damping observed in domain walls at room temperature in Fe_3O_4,[7] where none of the divalent iron is replaced by nickel, is larger than that observed in $(NiO)_{0.75}(FeO)_{0.25}Fe_2O_3$. Finally, as Wijn and van der Heide[17] have pointed out, and as (31) and (33) show more analytically, this mechanism is a very satisfactory explanation of the sharp change in domain wall relaxation frequency observed by Galt, Matthias, and Remeika.[29]

ACKNOWLEDGEMENTS

The author wishes to express his gratitude to many friends and colleagues for assistance with various aspects of this research. The crystals from which these samples were cut were obtained through Dr. G. W. Clark from the Linde Air Products Co. H. J. Williams has been of considerable help in observing the domain patterns. Most of the work of cutting the samples from bulk crystal and preparing them was done by J. A. Andrus, Mrs. M. R. Tiner, and R. E. Enz. The hysteresis loops were taken in collaboration with P. P. Cioffi and F. J. Dempsey. The special pulser used in obtaining the data was designed by H. R. Moore and built by H. G. Hopper. The chemical analyses were made by H. E. Johnson, J. F. Jensen, and J. P. Wright. Enlightening discussions were had with J. F. Dillon, Jr., C. Herring, A. N. Holden, B. T. Matthias, W. T. Read, H. J. Williams, and A. M. Clogston, who derived independently a result somewhat similar to that in (31). Useful comments were made on the manuscript by R. M. Bozorth, S. Millman and P. W. Anderson.

REFERENCES

1. Rado, Wright and Emerson, Phys. Rev., **80,** p. 273, 1950. Rado, Wright, Emerson and Terris, Phys. Rev., **88,** p. 909, 1952. G. T. Rado, Revs. Mod. Phys., **25,** p. 81, 1953. Welch, Nicks, Fairweather and Roberts, Phys. Rev., **77,** p. 403, 1950.
2. D. Polder and J. Smit, Revs. Mod. Phys., **25,** p. 89, 1953. J. J. Went and H. P. J. Wijn, Phys. Rev., **82,** p. 269, 1951. Wijn, Gevers and van der Burgt, Revs. Mod. Phys., **25,** p. 91, 1953. H. P. J. Wijn and H. van der Heide, Revs. Mod. Phys., **25,** p. 98, 1953. H. P. J. Wijn, Thesis, Leiden, 1953. Separaat 2092, N. V. Philips Gloeilampenfabrieken, Eindhoven, Holland.
3. H. J. Williams, Phys. Rev., **52,** p. 747, 1937. H. J. Williams and W. Shockley, Phys. Rev., **75,** p. 178, 1949. Williams, Bozorth and Shockley, Phys. Rev.,

75, p. 155, 1949. Williams, Shockley and Kittel, Phys. Rev., **80,** p. 1090, 1950. H. J. Williams, Bell Labs. Record **30,** p. 385, 1952.

3a. K. H. Stewart, Proc. Phys. Soc., **63A,** p. 761, 1950 and J. Phys. et Radium, **12,** p. 325, 1951.

4. K. J. Sixtus and L. Tonks, Phys. Rev., **42,** p. 419, 1932.

5. W. A. Yager and R. M. Bozorth, Phys. Rev., **72,** p. 80, 1947.

6. L. Landau and E. Lifshitz, Physik. Z. Sowjetunion, **8,** p. 153, 1935.

7. J. K. Galt, Phys. Rev., **85,** p. 664, 1952.

8. Galt, Andrus and Hopper, Revs. Mod. Phys., **25,** p. 93, 1953.

9. W. L. Bond, Phys. Rev., **78,** p. 646, 1950, Abstract I 10.

10. P. P. Cioffi, Phys. Rev., **67,** p. 200, 1945 and Rev. Sci. Instr., **21,** p. 624, 1950.

11. P. Weiss and R. Forrer, Ann. Phys., Series 10, **12,** p. 279, 1929. After the present work was completed, the author became aware of the extensive measurements of Pauthenet (Ann. Phys., Series 12, **7,** p. 710, 1952) on M_s in nickel ferrite and magnetite, among other materials. Interpolation between Pauthenet's values for these two materials suggests that the value of M_s we have used for $(NiO)_{0.75}\ (FeO)_{0.25}\ Fe_2O_3$ is about 6% too high at 445°K and 3% too low at 77°K, with intermediate errors between these temperatures and room temperature. Since, however, the accuracy of our data is not significantly better than this, and since our conclusions would be unaffected by any such changes, no correction has been made to our data.

12. R. Becker, J. Phys. et Radium, **12,** p. 332, 1951.

13. C. Kittel, Phys. Rev., **80,** p. 918, 1950; J. Phys. et Radium, **12,** p. 291, 1951.

14. C. Kittel, Revs. Mod. Phys., **21,** p. 541, 1949. See Equation 3.3.9. Since a wall perpendicular to the [100] direction in a crystal with a positive anisotropy energy constant is discussed in this reference, $g(\theta_0) = 0$ and is left out. The author is grateful to A. M. Clogston for pointing out the need for it in the present research. It was ignored in References 7 and 8 with the result that the values given for λ in those references were somewhat in error. Correct values are given in Table I.

15. E. J. W. Verwey and J. H. de Boer, Rec. Trav. Chim., **55,** p. 531, 1936. E. J. W. Verwey and P. W. Haaymann, Physica, **8,** p. 979, 1941. Verwey, Haaymann and Romeijn, J. Chem. Phys., **15,** p. 181, 1947.

16. M. E. Fine and N. T. Kenny, paper to be published.

17. H. P. J. Wijn and H. van der Heide, Revs. Mod. Phys., **25,** p. 99, 1953. H. P. J. Wijn, Thesis, Leiden, 1953. Separaat 2092, N. V. Philips Gloeilampenfabrieken, Eindhoven, Holland.

18. The author wishes to acknowledge a conversation with B. T. Matthias in which this mechanism was independently suggested in connection with the present research.

19. J. L. Snoek, New Developments in Ferromagnetic Materials, Elsevier, 1947.

20. It should be mentioned that Néel (J. Phys. et Radium **12,** p. 339, 1951; **13,** p. 249, 1952) has suggested that the after-effect losses discussed by Snoek[19] in connection with the diffusion of carbon and oxygen in iron arise from an anisotropy relaxation. Néel's analysis, however, leads him to predict zero loss for large motions of a 180° domain wall, which is contrary to our experimental results. We suggest that he is led to an erroneous result because he allows the anisotropy energy itself to follow a relaxation of the form of Equation (18), whereas kinetic losses of this sort are due to the relaxation of one of two conjugate thermodynamical variables whose *product* is an energy. In our case these variables are the torque on the magnetization due to anisotropy, and the angle of rotation of the magnetization. It is this torque which satisfies the relaxation equation.

21. C. Herring and C. Kittel, Phys. Rev., **81,** p. 869, 1951. See Equation 5.

22. L. R. Bickford, Jr., Phys. Rev., **78,** p. 449, 1950.

23. C. Kittel, Phys. Rev., **76,** p. 743, 1949.

24. Galt, Yager and Merritt, Phys. Rev., **93,** p. 1119, 1954. A more detailed description of this work is in preparation.
25. Yager, Galt, Merritt and Wood, Phys. Rev., **80,** p. 744, 1950. See Equation (A-6). The λ of the present paper is equal to $\gamma \alpha M_s$ in the notation of this reference.
26. N. Bloembergen and S. Wang, Phys. Rev., **93,** p. 72, 1954.
27. D. W. Healy, Jr., Phys. Rev., **86,** p. 1009, 1952.
28. G. T. Rado and J. R. Weertman, Phys. Rev., **94,** p. 1386, 1954.
29. Galt, Matthias and Remeika, Phys. Rev., **79,** p. 391, 1950.